Received: October 18, 2021. Revised: December 20, 2021.

International Journal of
Intelligent Engineering & Systems

http://www.inass.org/

MIFOCAT: A Unified Loss Function for Robust Myocardium Segmentation in Short-Axis Cine Cardiac Magnetic Resonance Images

Riandini[1], Fransiska Sisilia Mukti[1], Andria Arisal[2], Bambang Setiadi[2], Eko Mulyanto Yuniarno[1,3], I Ketut Eddy Purnama[1,3], Eko Setijadi[1], Mauridhi Hery Purnomo[1,3]*

[1]Department of Electrical Engineering, Institut Teknologi Sepuluh Nopember, Surabaya, 60111, Indonesia
[2]National Research and Innovation Agency, West Java, Bandung, 40135, Indonesia
[3]Department of Computer Engineering, Institut Teknologi Sepuluh Nopember, Surabaya, 60111, Indonesia
* Corresponding author's Email: hery@ee.its.ac.id

Abstract: Accurate segmentation of the myocardium from cardiac magnetic resonance imaging (MRI) plays a vital role in cardiac diagnosis and treatment planning. However, the task remains challenging due to anatomical variability, class imbalance, and subtle boundary delineations. This paper introduces MIFOCAT, a unified loss function designed to enhance myocardium segmentation accuracy in deep learning frameworks. MIFOCAT integrates Mean Squared Error (MSE, given alias as MI), Focal Loss (FO), and Categorical Cross-Entropy (CAT) to simultaneously address distribution, region, and boundary discrepancies in cardiac image segmentation. The proposed approach was evaluated using U-Net and TransUNet architectures on the ACDC 2017 dataset. A comprehensive ablation study demonstrated that combining the three loss components significantly improved segmentation fidelity and training stability. The U-Net model trained with MIFOCAT achieved the best results, with a Validation Intersection over Union (Val IoU) of 89.11% and Validation Accuracy (Val Acc) of 99.46%, surpassing models trained with single or traditional loss functions. In addition, the U-Net configuration required a shorter training time than TransUNet while maintaining superior precision. These findings confirm that MIFOCAT provides an effective and robust optimization strategy for deep learning-based cardiac MRI segmentation.

Keywords: Myocardium segmentation, Cardiac MRI, Deep Learning, Loss function, MIFOCAT.

1. Introduction

Image segmentation plays a pivotal role in medical diagnostics, particularly through its application in cardiac magnetic resonance imaging (MRI) [1-9]. This technique is indispensable for the early detection and monitoring of heart diseases, providing detailed visualizations of the heart's structure and function. Segmentation's ability to accurately delineate anatomical structures and pathological conditions from cardiac MRIs is crucial for planning effective clinical interventions and improving patient outcomes [10-12].

Advancements in deep learning (DL) have significantly propelled the capabilities of medical imaging technologies. In cardiac MRI, precise segmentation of cardiac structures, such as the myocardium, is essential for assessing heart health and guiding treatment decisions. However, accurately segmenting two-dimensional (2D) cardiac MRIs is challenging. These include the intrinsic variability in cardiac structure sizes and shapes, as well as the presence of overlapping regions, which complicate the segmentation process [13,14]. Central to addressing these challenges is the implementation of effective loss functions within deep learning frameworks. These functions provide a mathematical basis for measuring the discrepancy between the predicted and actual images, guiding the model to focus on relevant features for accurate segmentation [15,16].

Received: October 18, 2021. Revised: December 20, 2021.

The significance of choosing an appropriate loss function cannot be overstated, as it influences the efficiency and effectiveness of the learning process. While useful for classification tasks, conventional loss functions, such as categorical cross-entropy often fail to address the nuances necessary for detailed and accurate cardiac segmentation. They tend to overlook subtle boundaries and spatial correlations, leading to less precise results [17,18]. Moreover, while mean squared error (MSE) reduces pixel-wise discrepancies, it can blur crucial details, diminishing the diagnostic value of the images [19,20]. Meanwhile, focal loss, designed to address the class imbalance by focusing on difficult examples, does not by itself ensure comprehensive accuracy across all regions of the myocardium, potentially overlooking easier yet clinically significant areas [21,22].

Addressing these limitations, we introduce MIFOCAT, a unified loss function that integrates Mean Squared Error (MSE which is given alias as MI), Focal Loss (FO), and Categorical Cross-Entropy (CAT) to optimize myocardium segmentation in short-axis (SAX) cine cardiac MRI. Each component of MIFOCAT contributes a complementary role: MSE minimizes pixel-level discrepancies and enforces spatial smoothness; Focal Loss mitigates class imbalance by emphasizing difficult-to-segment myocardial regions; and Categorical Cross-Entropy strengthens inter-class discrimination for accurate delineation of cardiac structures. By combining these complementary objectives within a single optimization framework, MIFOCAT enhances boundary precision, improves segmentation consistency across heterogeneous imaging conditions, and stabilizes convergence during network training.

The main contributions of this paper are threefold. First, we propose MIFOCAT as a unified and interpretable loss function that harmonizes pixel-level regression, region-level balance, and class-level discrimination by integrating MI, FO, and CAT. This formulation enables more stable and accurate optimization for myocardium segmentation tasks.

Second, we conduct a comprehensive experimental evaluation using two renowned encoder–decoder architectures, namely U-Net [17] and Trans-Unet [18], trained and validated on the publicly available ACDC 2017 cardiac MRI dataset [23]. Extensive ablation studies are performed to isolate and analyze the contribution of each loss component.

Third, we present empirical evidence that MIFOCAT significantly improves segmentation accuracy, boundary delineation, and training stability compared to conventional and single-component loss functions, while also reducing training time. Together, these contributions establish MIFOCAT as an effective and robust optimization strategy for deep learning–based cardiac MRI segmentation, advancing the reliability and clinical applicability of automated cardiac analysis.

The subsequent sections will detail the technical framework of this integration, present experimental results, and provide a comprehensive analysis of the innovative approach's impact on the field of medical image segmentation.

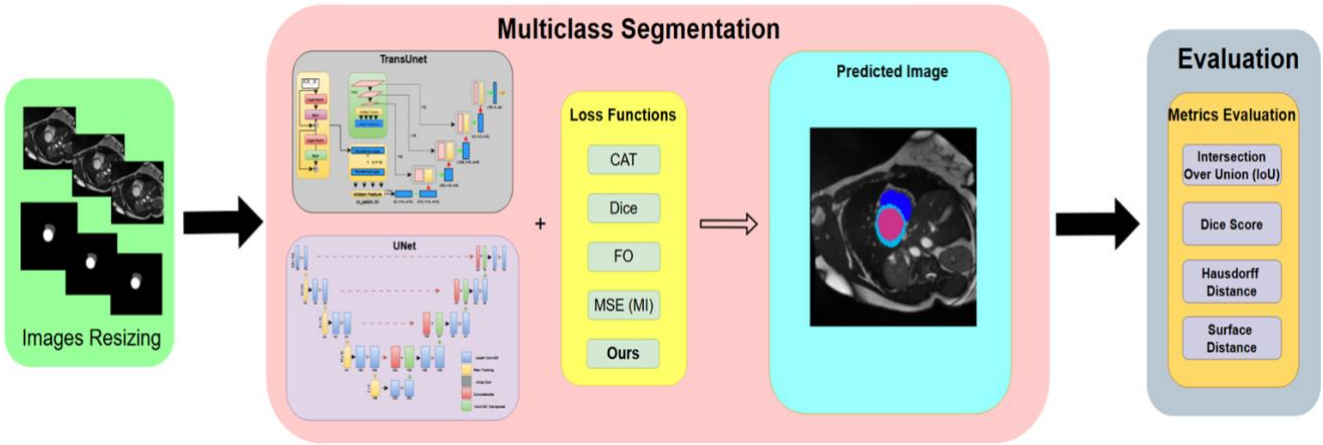

Figure 1. The proposed research workflow, beginning with image resizing, followed by multiclass segmentation using U-Net and TransUNet with various loss functions. The resulting predictions (where light blue denotes myocardium, pink represents the left ventricle, and dark blue indicates the right ventricle) are then evaluated using IoU, Dice, and distance-based metrics.

Received: October 18, 2021. Revised: December 20, 2021.

2. Materials and Methods

This section presents the overall methodological framework of the study. We first describe the dataset used for training and evaluation, followed by the preprocessing steps and segmentation scheme. The loss functions unification and evaluation criteria are also detailed in the subsequent subsections.

2.1 Dataset

This study utilized Automatic Cardiac Diagnosis Challenge (ACDC 2017) dataset [23]. It comprises short-axis (SAX) cine cardiac magnetic resonance images (MRI) acquired from routine clinical examinations at the University Hospital of Dijon, France. It provides comprehensive annotations for the segmentation of major cardiac structures and serves as a widely accepted benchmark for evaluating deep learning–based cardiac image segmentation algorithms.

2.2 Segmentation Scheme

Our segmentation approach is designed to assess the impact of various loss function combinations on the segmentation accuracy. The overall workflow is illustrated in Figure 1, beginning with a preprocessing stage in which all images are resized to ensure consistent input resolution. The normalized images are then processed using two segmentation architectures—U-Net and TransUNet—each combined with various loss functions to assess their influence on multiclass segmentation performance. The resulting predictions are visualized using class-specific colours: light blue for the myocardium, pink for the left ventricle, and dark blue for the right ventricle. Finally, the segmentation performance is evaluated using several metrics, including Intersection over Union (IoU), Dice coefficient, and distance-based measures that quantify the anatomical boundary accuracy. For segmentation, AI-based models derived from well-known Encoder-Decoder architectures, namely U-Net and Trans-Unet , were employed [9,24,25].

2.3 Loss Function Unification

Accurate segmentation of cardiac magnetic-resonance images requires a loss function that can handle three intrinsic challenges: large intensity variability among patients, severe class imbalance between myocardium and background, and subtle, low-contrast boundaries. Conventional single-component losses such as Categorical Cross-Entropy (CAT) or Dice Loss often emphasize only one of these aspects, leading to either blurred boundaries or biased region prediction.

To overcome these limitations, we introduce a unified loss formulation, termed MIFOCAT, that combines Mean Squared Error (MI), Focal Loss (FO), and Categorical Cross-Entropy (CAT) into a single optimization objective. Each component contributes complementary optimization behaviour: MI loss, L_{MI} , focuses on minimizing pixel-wise errors and enhancing segmentation accuracy, which is crucial for precise clinical diagnostics and treatment planning. It also helps in differentiating between closely situated cardiac structures by penalizing the discrepancies between predicted outputs and actual values. The formulation for MI loss is expressed as follows [32]:

$$L_{MI} = \frac{1}{n}\sum_{i=1}^{n}(y_i - \hat{y}_i)^2 \tag{1}$$

where y_i represents the actual segmentation map for the myocardial region in the i^{th} image, while $\hat{y}_i$, signifies the predicted segmentation map from the model for the same image. The variable n corresponds to the total number of images in the dataset. This loss function computes the average of the squared differences between the actual and predicted segmentation maps, offering a direct measure of the model's segmentation accuracy.

FO loss, L_{FO} adjusts the standard cross-entropy loss to prioritize hard-to-classify pixels, addressing the nuances and class imbalances prevalent in medical imaging, particularly in regions like the myocardium. This component is described by [31]:

$$L_{FO} = -\alpha_t\,(1 - p_t)^{\gamma}\,log\,(p_t) \tag{2}$$

Here, α_t acts as a weighting factor to ensure the myocardium class is not overshadowed by the more abundant background, while p_t indicates the probability that a pixel belongs to the myocardium class. The hyperparameter γ adjusts the loss contribution from each pixel based on its classification challenge, enhancing the model's accuracy in delineating myocardial boundaries. This is particularly significant in the context of medical image segmentation, where pixel-wise adjustments can help address issues related to class imbalance and boundary delineation [26, 27]. In this model, α and γ values are optimally set at 0.25 and 2, respectively, to focus on the most challenging aspects of myocardial segmentation

Received: October 18, 2021. Revised: December 20, 2021.

CAT loss, L_{CAT}, is employed to enhance the segmentation accuracy of various cardiac structures by aligning the predicted probabilities of pixel classification with their actual labels. The loss function is defined as [33]:

$$L_{CAT} = -\sum_{c=1}^{M} y_{o,c}\ log\left(p_{o,c}\right) \quad (3)$$

In this context, M represents the total number of classes involved in the segmentation process, including various cardiac tissues and backgrounds, with $M = 4$ for this study. The term $y_{o,c}$ is a binary indicator that verifies whether class c is the correct classification for pixel o, and $p_{o,c}$ denotes the predicted probability of the pixel o being classified under class c, as determined by the model. This formulation ensures a targeted approach to managing the complexities of cardiac segmentation.

The composite function for the MOFICAT loss, L_{uni}, is represented by:

$$L_{uni} = r_1 L_{MI} + r_2 L_{FO} + r_3 L_{CAT} \quad (4)$$

Here, L_{MI}, L_{FO}, and L_{CAT} are the MI, FO, and CAT loss components, respectively, with r_1, r_2, and r_3 serving as tunable hyperparameters

he proposed loss functions enhance segmentation outcomes by rectifying errors across various scales, from general distribution discrepancies to the precise delineation of specific boundaries.

2.4 Evaluation Criteria

The Intersection over Union (IoU) and the Mean Surface Distance (MSD). IoU [28]:

$$IoU = \frac{|n_S \cap n_{S'}|}{|n_S \cup n_{S'}|} = \frac{TP}{(TP+FP+FN)} \quad (5)$$

Meanwhile, MSD a precise measure of boundary accuracy critical for detailed anatomical and pathological evaluations [29]:

$$MSD = \frac{1}{n_S + n_{S'}}\left(\sum_{p=1}^{n_S} d(p,S') + \sum_{p'=1}^{n_{S'}} d(p',S)\right) \quad (6)$$

In practical applications, a lower MSD value indicates a closer alignment between the predicted and ground-truth boundaries, reflecting the model's ability to capture subtle structural variations and fine morphological details an essential aspect in cardiac imaging where millimeter-level discrepancies can lead to clinically significant interpretation differences. This metric, therefore, not only quantifies spatial precision but also serves as a critical benchmark for validating segmentation algorithms in sensitive diagnostic workflows.

These metrics together furnish a comprehensive assessment of the segmentation efficacy, underlining the practical implications of the MIFOCAT loss function in clinical imaging contexts.

3. Results and Discussion

This section presents the experimental results and analysis of the proposed cardiac MRI segmentation framework. We outline the implementation settings, including the computational environment and training configuration, followed by ablation results examining the effects of different loss-function combinations on U-Net and TransUNet. Performance is evaluated using accuracy- and overlap-based metrics, and the comparative analysis highlights the most effective loss-function configuration identified in this study..

3.1 Implementation Details

The neural network models developed in this study were implemented using TensorFlow 2.15 and Python 3.10. Experiments were conducted across two computing environments: (i) a Windows 10 workstation equipped with an Intel Core–based CPU (exact specifications not reported), used primarily for preliminary testing and code verification; and (ii) a Google Colab environment configured with the platform's standard GPU allocation, which served as the primary training environment.

The segmentation architectures followed a conventional encoder–decoder design, where each convolutional and deconvolutional block utilized a 3×3 kernel to preserve spatial detail while enabling robust feature extraction. Spatial resolution was reduced through 2×2 down-sampling operations applied at each encoder level, with symmetric up-sampling operations in the decoder to restore full-resolution predictions. All intermediate feature transformations employed the ReLU activation function [17], consistent with widely adopted practices in medical image segmentation.

Received: October 18, 2021. Revised: December 20, 2021.

Table 1. Segmentation evaluation performance (%) for U-Net and TransUNet using different loss functions on the validation set.

Model	Loss Function	Val Loss	Val Acc (%)	Val IoU (%)	Time (s)
U-net	Categorical Crossentropy (CAT)	0.0169	99.3532	86.9386	151.5306
	Dice Loss	0.0204	99.4609	89.0568	153.4167
	Focal Loss	0.0011	99.4118	88.5282	154.2675
	MSE + CAT	0.0147	99.4843	89.2694	153.3976
	MSE + Focal + CAT (MIFOCAT)	0.0016	99.4576	89.1112	156.9146
	MSE + Dice + CAT	0.0233	99.4464	88.8990	153.5602
TransUNet	Categorical Crossentropy (CAT)	0.0029	99.4980	89.4946	10790.0169
	Dice Loss	0.0219	99.4814	88.6938	10765.5535
	Focal Loss	0.02197	89.7287	58.9551	10698.0039
	MSE + CAT	0.0175	99.4016	87.8197	10088.2755
	MSE + Focal + CAT (MIFOCAT)	0.0020	99.3926	87.3015	9738.9877
	MSE + Dice + CAT	0.0365	99.2807	85.6630	10081.8302

Model optimization was performed using the ADAM optimizer with a batch size of 8 and an initial learning rate of 1×10^{-3}. Training was conducted for 50 epochs across all model–loss configurations to ensure fair comparison. The models were trained using the proposed custom loss function described in Eq. (4), where the parameter γ in the focal component (Eq. 2) was fixed at $\gamma = 2$ following recommendations from prior work [30]. This setup ensures stable gradient behavior during optimization and provides a consistent training protocol for evaluating the impact of different loss-function combinations.

3.2 Ablation Study

Based on the results presented in Table 1, we compared the performance of the U-Net and TransUNet architectures. Our evaluation included several key loss functions, such as Categorical Cross-Entropy (CAT), Dice Loss, and Focal Loss, as well as combinations including Mean Squared Error (MSE). Overall, the U-Net architecture demonstrated a more promising balance of performance and efficiency. We found that the combined loss function of Mean Squared Error (MSE), Focal Loss, and Categorical Cross-Entropy (CAT) (which we designate as MIFOCAT) yielded the most optimal results for the U-Net model.

This configuration achieved a Validation Intersection over Union (Val IoU) of 89.1112%. Although its Validation Accuracy (Val Acc) of 99.4576% was not the absolute highest (being slightly outperformed by another combination), the high Val IoU score is more significant. It indicates that the MIFOCAT configuration provides a precise delineation of the target segmentation regions, which is a more critical metric for this task.

For the TransUNet architecture, the standard Categorical Cross-entropy loss function achieved the highest Val IoU for that model (89.4946%). However, this superior score came at an extreme computational cost (10790.0s).

In a direct comparison, our U-Net with MIFOCAT, while posting a slightly lower but highly competitive IoU (89.1112%), was significantly faster to train (156.9s). Given this dramatic advantage in efficiency for a minimal trade-off in segmentation accuracy, we selected the U-Net with MIFOCAT (denoted as "UNet Ours") as the optimal model for further investigation across various pathological subgroups (as shown in Figure 1).

The model exhibited excellent and stable performance for Left Ventricle segmentation, achieving high Mean IoU and Mean Dice scores consistently across all five patient conditions. Performance on myocardium segmentation was also robust, as detailed in Figure 2. The overlap-based metrics (Mean IoU and Mean Dice) were strongest and most stable for the HCM (Hypertrophic Cardiomyopathy) and NOR (Normal) groups, showing high median scores and tight distributions.

Received: October 18, 2021. Revised: December 20, 2021.

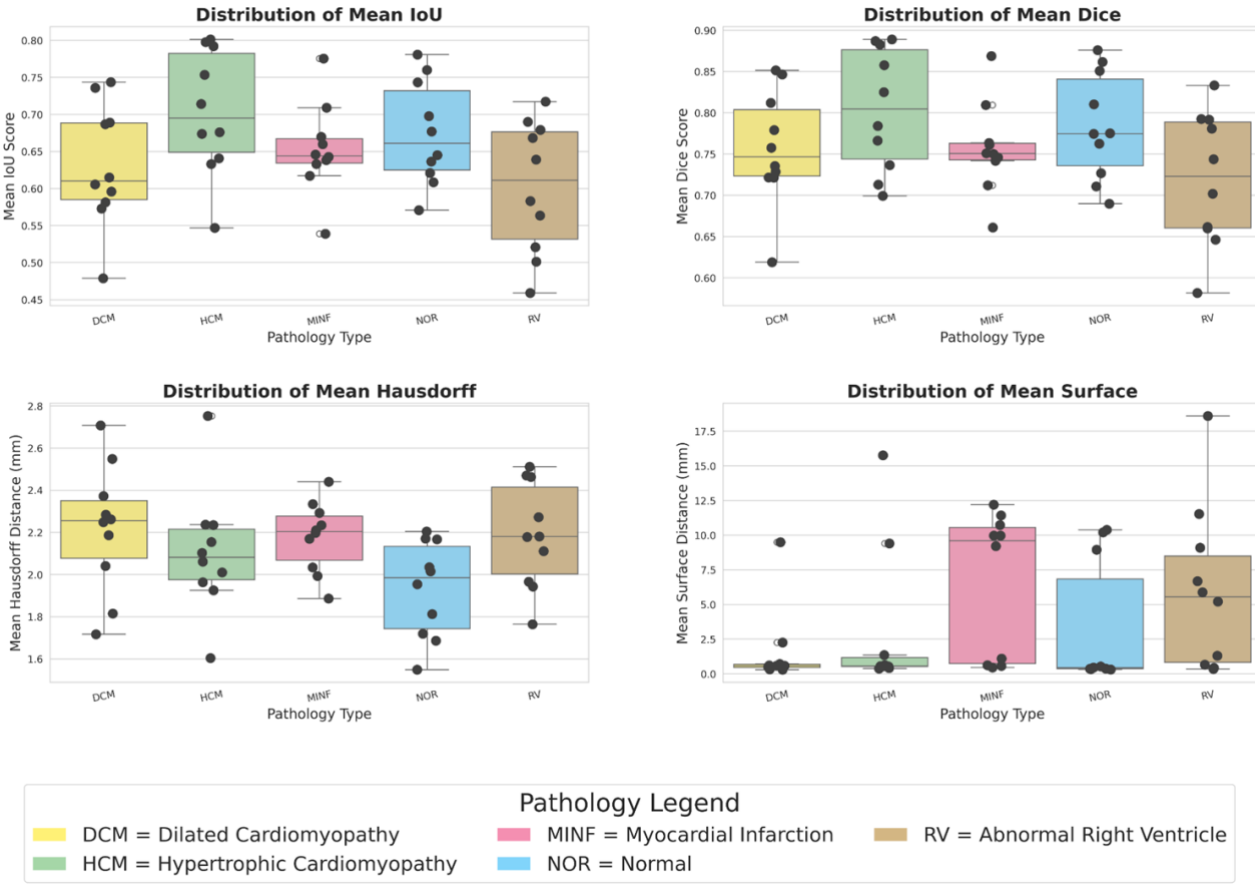

Figure 2 Comparison of segmentation metrics for the myocardium using our proposed UNet (Ours) model. The box plots illustrate the distribution of Mean IoU, Mean Dice, Mean Hausdorff Distance, and Mean Surface Distance across five patient conditions: DCM (Dilated Cardiomyopathy), HCM (Hypertrophic Cardiomyopathy), MINF (Myocardial Infarction), NOR (Normal), and RV (Abnormal Right Ventricle).

Conversely, the distance-based metrics revealed challenges in specific pathologies. We observed a significantly higher median and wider variance for Mean Surface Distance in cases of myocardial infarction (MINF). This suggests that while the model generally identifies the correct area, it struggles to precisely delineate the complex boundaries in these specific regions. The RV (Abnormal Right Ventricle) pathology also presented difficulties, showing high variability and lower median scores across all metrics.

The Right Ventricle emerged as the most challenging structure to segment, manifesting lower IoU/Dice scores and a conspicuously higher incidence of distance errors. This comprehensive analysis substantiates the model's overall effectiveness, particularly for the Left Ventricle, while simultaneously underscoring the inherent difficulty of segmenting the more complex and variable Right Ventricle structure.

To complement our quantitative metrics, we conducted a qualitative analysis, presented in Table 2 and 3. These tables provide a visual comparison of the final prediction masks from both U-Net and TransUNet, juxtaposed against the original image and the ground-truth label for a representative test slice, allowing a clearer assessment of each model's ability to preserve anatomical boundaries and accurately delineate the myocardium.

This visual inspection reveals a key observation: the TransUNet architecture is highly sensitive to the choice of loss function. Pure Focal Loss (FO) led to a near-complete segmentation failure, with the model unable to identify the target structures. Dice-based losses—both pure Dice Loss and the MSE + Dice + CAT combination—also introduced substantial false-positive artifacts, incorrectly segmenting regions outside the heart. In contrast, the proposed MIFOCAT (MSE + Focal + CAT) consistently produced clean, accurate, and artifact-free segmentations for both U-Net and TransUNet, closely matching the ground truth and demonstrating stronger robustness across configurations.

Received: October 18, 2021. Revised: December 20, 2021.

Table 2. Example of comparative myocardial segmentation results in patients with myocardial infarction (MINF). Light blue regions indicate the segmented myocardium, while red arrows highlight areas of inaccurate or misclassified predictions, illustrating typical segmentation challenges encountered in pathological cases.

IMAGE		
Origin + Groundtruth(GT)	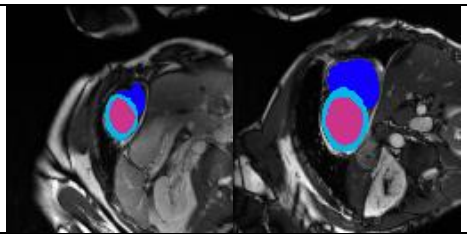	
RESULTS		
Loss Functions	**Unet**	**TransUnet**
Categorical Crossentropy (CAT)	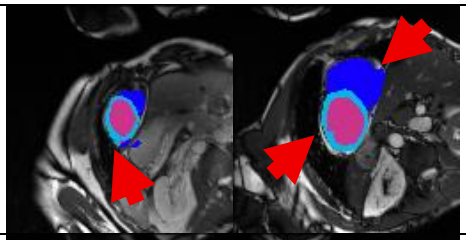	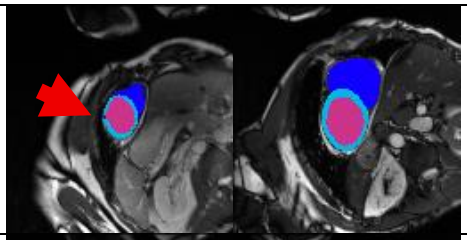
Dice Loss	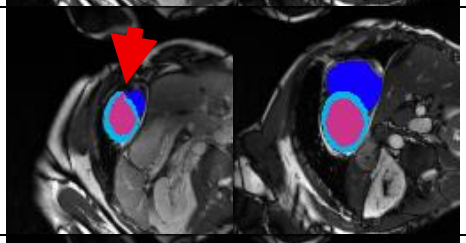	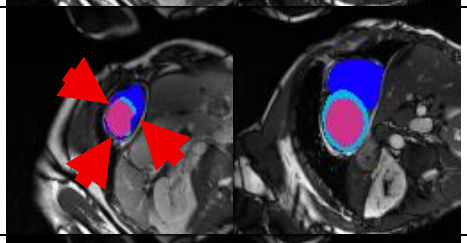
Focal Loss (FO)	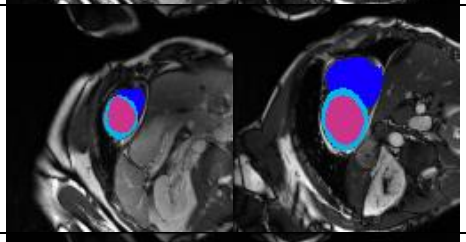	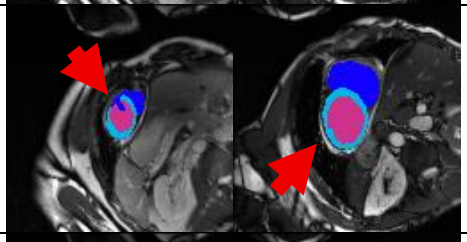
MSE + CAT	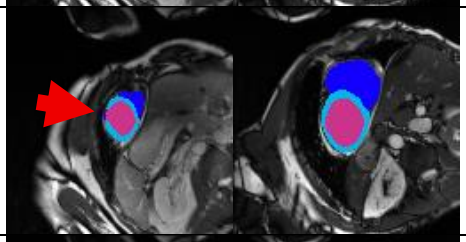	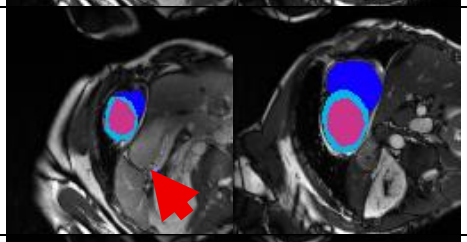
MSE + Focal + CAT (MIFOCAT)	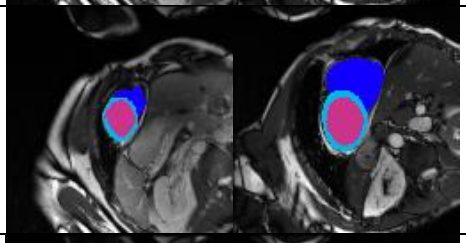	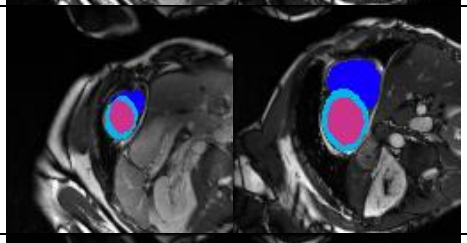
MSE + Dice + CAT	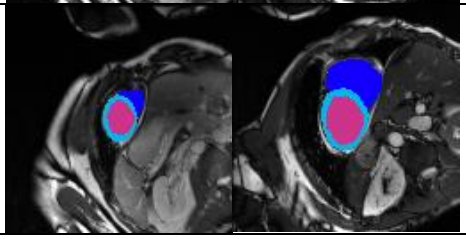	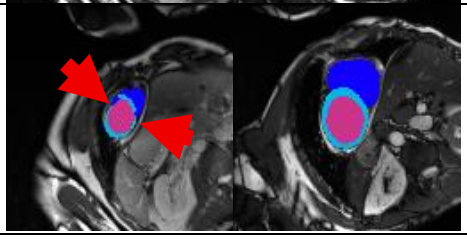

Received: October 18, 2021. Revised: December 20, 2021.

Table 3. Example of comparative myocardial segmentation results in healthy/normal (NOR) patients. The light-blue regions denote correctly segmented myocardium under normal cardiac morphology. Red arrows highlight subtle inaccuracies in the predicted masks, illustrating segmentation errors that may still arise even in structurally normal heart images.

IMAGE		
Origin + Groundtruth(GT)	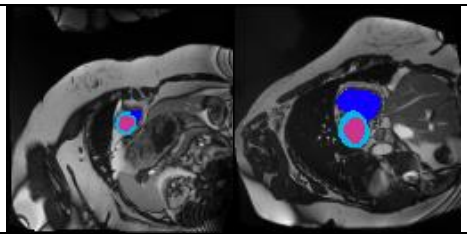	
RESULTS		
Loss Functions	Unet	TransUnet
Categorical Crossentropy (CAT)	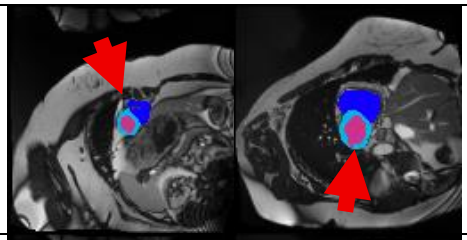	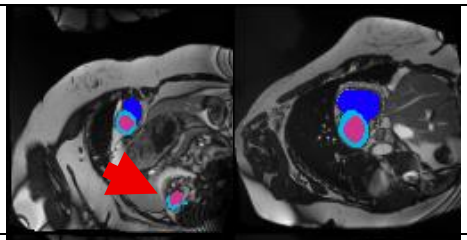
Dice Loss	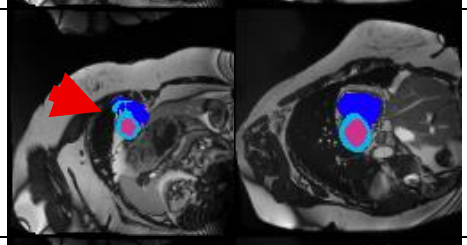	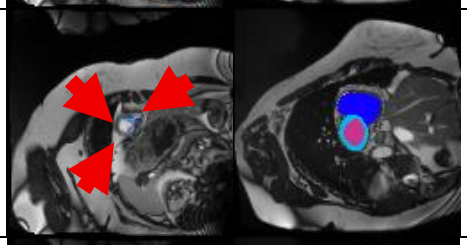
Focal Loss (FO)	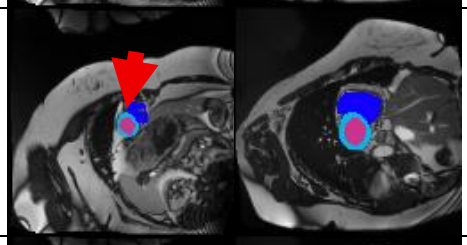	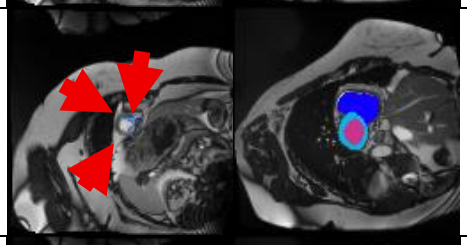
MSE + CAT	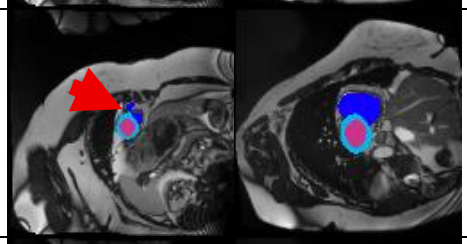	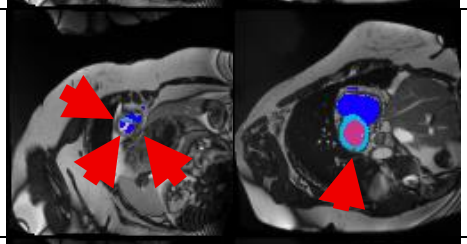
MSE + Focal + CAT (MIFOCAT)	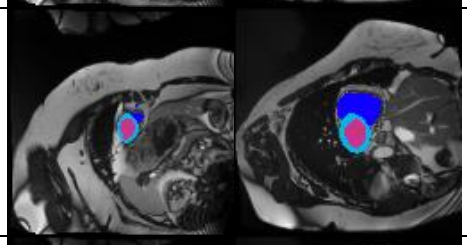	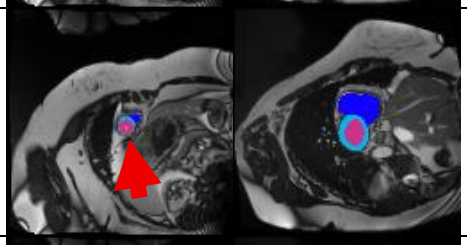
MSE + Dice + CAT	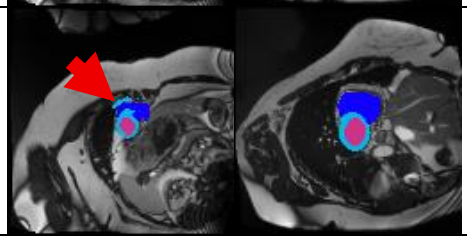	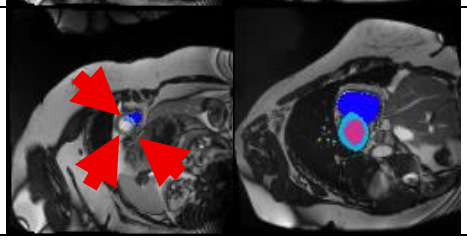

Received: October 18, 2021. Revised: December 20, 2021.

In contrast, the U-Net architecture appeared visually more stable and robust across most loss function configurations. While it also produced minor artifacts (e.g., small false positives) when using pure Dice Loss, it did not suffer the same catastrophic failures as TransUNet. This qualitative evidence strongly corroborates our quantitative findings, underscoring MIFOCAT's reliability and its ability to prevent the instability and prediction errors observed in other loss function setups

4. Conclusion

This study introduced and validated MIFOCAT, a unified loss function combining Mean Squared Error, Focal Loss, and Categorical Cross-Entropy to address key challenges in myocardial segmentation from SAX cine cardiac MRI. Through an ablation study using U-Net and TransUNet, the proposed loss function consistently improved segmentation performance. U-Net, paired with MIFOCAT, achieved the best results, with a Val IoU of 89.11% and a Validation Accuracy of 99.46%, outperforming TransUNet (Val IoU 87.30%). Additionally, U-Net required substantially shorter training time, highlighting its practical efficiency for this task.

Conflicts of Interest

All authors declare no conflict of interest.

Author Contributions

Conceptualization, Riandini, F.S. Mukti, A. Arisal, and B. Setiadi; Methodology, Riandini and I.K.E. Purnama; Software, Riandini and B. Setiadi; Validation, I.K.E. Purnama and M.H. Purnomo; Formal Analysis, Riandini and E.M. Yuniarno; Resources, I.K.E. Purnama and E. Setijadi; Data Curation, Riandini, F.S. Mukti, A. Arisal, B. Setiadi, and I.K.E. Purnama; Writing—Original Draft, Riandini, A. Arisal, and B. Setiadi; Writing—Review & Editing, E.M. Yuniarno and I.K.E. Purnama; Visualization, Riandini and B. Setiadi; Supervision, E.M. Yuniarno, I.K.E. Purnama, E. Setijadi, and M.H. Purnomo. All authors approved the final manuscript.

Acknowledgments

This work was supported by the Computer Engineering Department, Institut Teknologi Sepuluh Nopember (ITS) through research funding under contract number 2193/PKS/ITS/2025, granted under The Institutional Development scheme.

References

[1] N. Zaki, W. Qin, and A. Krishnan, "Graph-based methods for cervical cancer segmentation: Advancements, limitations, and future directions," AI Open, vol. 4, pp. 42–55, Jan. 2023.

[2] P. Khosravi, S. Mohammadi, F. Zahiri, M. Khodarahmi, and J. Zahiri, "AI‐Enhanced Detection of Clinically Relevant Structural and Functional Anomalies in MRI: Traversing the Landscape of Conventional to Explainable Approaches," Journal of Magnetic Resonance Imaging, vol. 60, no. 6, pp. 2272–2289, 2024.

[3] K. Sivakumar, S. Lavanya, K. Himanandini, and V. Keerthana, "A Unified Automated Segmentation Technique for the Left Ventricle Segmentation in Cardiac MRI," IOP Conference Series: Materials Science and Engineering, vol. 993, no. 1, pp. 012068, 2020.

[4] Z. Liu, K. Kainth, A. Zhou, T. Deyer, Z. A. Fayad, H. Greenspan, and X. Mei, "A review of self‐supervised, generative, and few‐shot deep learning methods for data‐limited magnetic resonance imaging segmentation," NMR in Biomedicine, vol. 37, no. 8, 2024.

[5] H. Cui, M. Piao, X. Huang, X. Zhu, H. Ma, and Y. Peng, "Advancing cardiac MRI multi‐structure segmentation: A semi‐supervised multidimensional consistency constraint learning network," Medical Physics, vol. 52, no. 7, 2025.

[6] M. A. Zuluaga, M. J. Cardoso, and S. Ourselin, "Automatic Right Ventricle Segmentation using Multi-Label Fusion in Cardiac MRI," Preprint, 2020.

[7] N. Das and S. Das, "Cardiac MRI Segmentation Using Deep Learning," Preprint, 2022.

[8] Z. Chen, J. Bai, and Y. Lu, "Dilated convolution network with edge fusion block and directional feature maps for cardiac MRI segmentation," Frontiers in Physiology, Vol. 14, 2023.

[9] T. Geroski, N. Filipović, and A. Amini, "Segmentation of ACDC challenge cardiac MRI dataset across diverse neural network architectures," Preprint, pp. 75, 2025.

[10] G. Litjens, F. Ciompi, J. Wolterink, B. Vos, T. Leiner, J. Teuwenet al., "State-of-the-art deep learning in cardiovascular image analysis", JACC: Cardiovascular Imaging, Vol. 12, No. 8, pp. 1549-1565, 2019.

Received: October 18, 2021. Revised: December 20, 2021.

[11] J. Wang, H. Huang, C. Chen, W. Ma, Y. Huang, & X. Ding, "Multi-sequence cardiac mr segmentation with adversarial domain adaptation network", Lecture Notes in Computer Science, pp. 254-262, 2020.

[12] E. Abouei, S. Pan, M. Hu, A. Kesarwala, J. Zhou, J. Roperet al., "Cardiac mri segmentation using block-partitioned transformer with global-local information integration", Medical Imaging 2024: Clinical and Biomedical Imaging, 2024.

[13] S. Cai, Y. Lu, B. Li, Q. Gao, L. Xu, X. Huet al., "Segmentation of cardiac tissues and organs for ccta images based on a deep learning model", Frontiers in Physics, Vol. 11, 2023.

[14] J. Wang, S. Wang, W. Liang, N. Zhang, & Y. Zhang, "The auto segmentation for cardiac structures using a dual‐input deep learning network based on vision saliency and transformer", Journal of Applied Clinical Medical Physics, Vol. 23, No. 5, 2022.

[15] R. Upendra, B. Wentz, R. Simon, S. Shontz, & C. Linte, "Cnn-based cardiac motion extraction to generate deformable geometric left ventricle myocardial models from cine mri", Lecture Notes in Computer Science, pp. 253-263, 2021.

[16] M. Yeung, E. Sala, C. Schönlieb, & L. Rundo, "Unified focal loss: generalising dice and cross entropy-based losses to handle class imbalanced medical image segmentation", Computerized Medical Imaging and Graphics, Vol. 95, pp. 102026, 2022.

[17] O. Ronneberger, P. Fischer, and T. Brox, "U-net: Convolutional networks for biomedical image segmentation," in Lecture Notes in Computer Science, Vol. 9351, pp. 234–241, 2015.

[18] C. Chen, C. Qin, H. Qiu, G. Tarroni, J. Duan, W. Baiet al., "Deep learning for cardiac image segmentation: a review", Frontiers in Cardiovascular Medicine, Vol. 7, 2020.

[19] J. Ma et al., "Loss odyssey in medical image segmentation," Med. Image Anal., Vol. 71, 2021.

[20] K. Hammouda, F. Khalifa, H. Abdeltawab, A. Elnakib, G. Giridharan, M. Zhuet al., "A new framework for performing cardiac strain analysis from cine mri imaging in mice", Scientific Reports, Vol. 10, No. 1, 2020.

[21] B. H. Menze et al., "The Multimodal Brain Tumor Image Segmentation Benchmark (BRATS)," IEEE Trans. Med. Imag., Vol. 34, No. 10, pp. 1993–2024, 2015.

[22] D. Vigneault, W. Xie, C. Ho, D. Bluemke, & J. Noble, "Ω-net (omega-net): fully automatic, multi-view cardiac mr detection, orientation, and segmentation with deep neural networks", Medical Image Analysis, Vol. 48, pp. 95-106, 2018.

[23] O. Bernard et al., "Deep Learning Techniques for Automatic MRI Cardiac Multi-Structures Segmentation and Diagnosis: Is the Problem Solved?," IEEE Trans. Med. Imag., Vol. 37, No. 11, pp. 2514–2525, 2018.

[24] A. Bhan, P. Mangipudi, & A. Goyal, "Cardiac mri segmentation using efficient resnext-50-based iei level set and anisotropic sigmoid diffusion algorithms", International Journal of Image and Graphics, Vol. 24, No. 06, 2022.

[25] Y. Gu, Z. Piao, & S. Yoo, "Sthardnet: swin transformer with hardnet for mri segmentation", Applied Sciences, Vol. 12, No. 1, pp. 468, 2022.

[26] M. Yeung, E. Sala, C. Schönlieb, & L. Rundo, "Unified focal loss: generalising dice and cross entropy-based losses to handle class imbalanced medical image segmentation", Computerized Medical Imaging and Graphics, Vol. 95, pp. 102026, 2022.

[27] K. Wong, M. Moradi, H. Tang, & T. Syeda-Mahmood, "3d segmentation with exponential logarithmic loss for highly unbalanced object sizes", Lecture Notes in Computer Science, pp. 612-619, 2018.

[28] H. Rezatofighi, N. Tsoi, J. Gwak, A. Sadeghian, I. Reid, and S. Savarese, "Generalized Intersection over Union: A Metric and A Loss for Bounding Box Regression," 2019.

[29] A. A. Taha and A. Hanbury, "Metrics for evaluating 3D medical image segmentation: analysis, selection, and tool," BMC Medical Imaging, Vol. 15, No. 29, 2015.

[30] T. Y. Lin, P. Goyal, R. Girshick, K. He, and P. Dollar, "Focal Loss for Dense Object Detection," IEEE Trans. Pattern Anal. Mach. Intell., Vol. 42, No. 2, pp. 318–327, 2020.

[31] T.-Y. Lin, P. Goyal, R. Girshick, K. He, and P. Dollar, "Focal Loss for Dense Object Detection," 2017 IEEE International Conference on Computer Vision (ICCV), 2017.

[32] K. Das, J. Jiang, and J. N. K. Rao, "Mean squared error of empirical predictor," The Annals of Statistics, Vol. 32, No. 2, 2004.

[33] A. Mao, M. Mohri, and Y. Zhong, "Cross-Entropy Loss Functions: Theoretical Analysis and Applications," arXiv.org, 2023.

Received: October 18, 2021. Revised: December 20, 2021.

----- Please read the following conditions carefully -----

Before Submission

Please review the following information before submitting your manuscript. It is not necessary to include the text below in your paper.

Please confirm the following terms.

- ☑ **The review process of the International Journal of Intelligent Engineering and Systems (IJIES) consists of two stages: the first review and the second review. Each stage typically requires about two weeks to complete. Accepted papers will be published approximately two months after acceptance.**
  - **Please ensure that your initial submission is formatted in a two-column layout to clearly indicate the length of the manuscript.**

- ☑ **The paper length is more than 8 pages.**
  - **If the page length exceeds 10 pages, the extra page charge USD50 per extra page will be requested.)**
  - **An additional fee of USD 100 will be charged if authors do not use the prescribed formatting template, "IJIES_Format.docx".)**

- ☑ **The paper is not Survey Research (or Review paper).**

- ☑ **All figures/tables/equations are original works.**

- ☑ **All figures/tables are clear.**
  (The letter of figures is 10-point Times New Roman.)

- ☑ **The full name of authors is given in your manuscript.**

- ☑ **Submission of a manuscript to the International Journal of Intelligent Engineering and Systems (IJIES) signifies that the work has not been previously published, is not under copyright elsewhere, and is not currently under consideration by any other publication. The authors declare no conflict of interest.**

By submitting a manuscript, the authors are deemed to have agreed to the above terms and conditions.

Received: October 18, 2021. Revised: December 20, 2021.

From May 18, 2025

Information of IJIES Awards

Excellent Citation Award

The Excellent Citation Award of IJIES is granted to an individual or group who has made significant and important contributions to the International Journal of Intelligent Engineering and Systems (IJIES).

Nomination criteria:

More than 30 citation counts are necessary **within a year** after paper publication.

How to apply "Excellent Citation Award":

To proof your citation counts, please submit "Author search result" of "Scopus Preview" to IJIES office. (Check https://www.scopus.com/)

* The citation is counted by using "Scopus" database.

For Excellent Citation Award recipients:

Honorary certificate will be provided to an individual or group.

Outstanding Citation Award

The Outstanding Citation Award of IJIES is granted to an individual or group who has made significant and important contributions to the International Journal of Intelligent Engineering and Systems (IJIES).

Nomination criteria:

More than 50 citation counts are necessary within **three years** after paper publication.

How to apply "Outstanding Citation Award":

To proof your citation counts, please submit "Author search result" of "Scopus Preview" to IJIES office. (Check https://www.scopus.com/)

* The citation is counted by using "Scopus" database.

For Outstanding Citation Award recipients:

Honorary certificate will be provided to an individual or group.

Received: October 18, 2021. Revised: December 20, 2021.

----- Please read the following conditions carefully -----

Fast Publication Service

In response to numerous requests from our valued authors, we are pleased to introduce the "Fast Publication Service."

While the International Journal of Intelligent Engineering and Systems (IJIES) typically publishes accepted manuscripts within two months, this new service offers an expedited publication timeline. Authors who choose this option will have their accepted papers published within one month of acceptance.

Please confirm the following terms.

- ☑ **Accepted papers under this service will be published within ONE month of acceptance. Additionally, the camera-ready version will be sent to the authors within approximately TWO weeks following the acceptance of the paper.**
- ☑ **The "Fast Publication Service" is available for a fee of USD 50.**

After completing the required information in the form below, please submit it via your "MyPage".

Paper ID	
Paper Title	MIFOCAT: A Unified Loss Function for Robust Myocardium Segmentation in Short-Axis Cine Cardiac Magnetic Resonance Images
Full Name of Corresponding Author	Riandini, Fransiska Sisilia Mukti, Andria Arisal, Bambang Setiadi, Eko Mulyanto Yuniarno, I Ketut Eddy Purnama, Eko Setijadi, Mauridhi Hery Purnomo
Organisation	Institut Teknologi Sepuluh Nopember, Surabaya, Indonesia
E-mail	hery@ee.its.ac.id

Once this form has been submitted, a PayPal payment request will be issued to the email address indicated above. Following confirmation of payment, the accepted article will be published on the website within one month.

Received: October 18, 2021. Revised: December 20, 2021.

Application for Amendment Services

In response to numerous requests from our valued authors, we are pleased to introduce the "Amendment Services."

Please confirm the following terms.

- ☐ **If you wish to request an amendment to an already published paper, please complete the form below and submit it to the IJIES Office. A correction fee of USD 100 will be charged, and only papers published on the INASS website are eligible for amendment.**
- ☐ **Please note that we cannot accept any revisions that result in an increase in the number of pages, as this may affect the layout and pagination of other authors' papers. Furthermore, if the editorial office determines that the requested amendment involves data fabrication or any other form of misconduct, the application will be rejected.**

After completing the required information in the form below, please submit it to the Editorial Office.

Paper ID	
Paper Title	
Full Name of Corresponding Author	
Organisation	
E-mail	
Kindly describe in detail the specific content you are requesting to be amended.	

Once this form has been submitted, a PayPal payment request will be issued to the email address indicated above. Following confirmation of payment, the revised article will be published on the website within one month.